Single-molecule FRET and tracking of transfected biomolecules: multi-dimensional protein dynamics in living cells

Abhinaya Anandamurugan[1], Antonia Eidloth[1], Philipp Wortmann[1], Lukas Schrangl[4], Fernando Aprile-Garcia[2], Chenyang Lan[1], Ritwick Sawarkar[5], Gerhard J. Schütz[4] and Thorsten Hugel[1,3*]*

1. Institute of Physical Chemistry, University of Freiburg, Albertstr. 21, 79104 Freiburg, Germany

2. Max-Planck-Institute for Immunobiology and Epigenetics, Stübeweg 51, 79108 Freiburg, Germany

3. Signalling research centers BIOSS and CIBSS, University of Freiburg, Germany

4. Institute of Applied Physics, TU Wien, 1060 Vienna, Austria.

5. MRC Toxicology Unit, University of Cambridge, Cambridge, UK.

**contact: Abhinaya.Anandamurugan@pc.uni-freiburg.de; Thorsten.Hugel@pc.uni-freiburg.de*

Abstract:

Proteins in cells exhibit conformational dynamics, equally influenced by dynamic interactions with other biomolecules and their spatial variations, which can be induced by the protein`s compartment. Altogether this multi-dimensional dynamic is difficult to measure *in cellula*, because of limitations in instrumentation, fluorescence methodologies and the difficulty to track freely diffusing molecules. Here, we present a bottom-up engineering approach, which allows us to track transfected proteins *in cellula* and analyze time-resolved single-molecule FRET efficiencies. This has been achieved by alternating laser excitation (ALEX) based three-channel (donor, acceptor and FRET intensity) tracking with a live-cell HILO microscope. Unexpectedly, we find that the heat shock protein Hsp90 shows different conformational populations *in vitro* and *in cellula*. Moreover, Hsp90's conformational states depend on the localization within the cell, which is demonstrated by comparing a physical (microinjection) and a biological (SLO) transfection method. FRET-TTB (*Tracking of Transfected Biomolecules*) opens the path to study protein conformational dynamics of transfected and native biomolecules *in cellula*, including time-resolved cellular localization.

Introduction:

Investigation of protein structure and dynamics *in vitro* has largely enhanced our understanding of proteins and their interactions. Now we need to determine how protein structure, dynamics and interactions are affected by the crowded non-equilibrium environment of living cells, ideally in a spatially resolved way. A promising direction is to quantify the conformational dynamics of single proteins in living cells with single-molecule FRET. For some membrane proteins this has already been successfully achieved[1], but not for soluble proteins that can be in many compartments or in the cytosol within the cell. The central problem to achieve this in mammalian cells is to track single molecules showing conformational dynamics and to disentangle the effect of the microenvironment on the fluorophores from protein conformational states. To understand distance dependent conformational changes single molecule FRET (smFRET) has been most reliable in detecting changes less than 10 nm[2]. There have been three main types of methods employed to study conformational changes. First, lifetime photon burst[3]. Second, sensitized emission (two channel – Donor and FRET) measurements[4,5,6]. Third, ALEX-based methods involving either confocal (photon burst) microscopy[7] or total internal reflection (TIR) / Highly Inclined Laminated Optical Sheet (HILO) microscopy (intensity traces)[1]. Lifetime measurements provide rich information on molecular decay time and are highly sensitive to local environment, but they are blind towards bleaching of individual emitters and thus do not give stoichiometry of interacting species[8]. Sensitized emission measurements, mainly used to study membrane proteins, discount the effect of microenvironment on fluorophore. ALEX-based time-resolved confocal TCSPC techniques, while able to detect stoichiometry, can hardly be used to study

long term interactions or conformational changes on the timescale of seconds[9]. ALEX-based fluorescence intensity measurements, which provide stoichiometry information, would be ideal, but they have not been employed for cytosolic proteins due to difficulties in localizing both fluorophores and tracking them while protein conformational changes happen. Here we present a method that can disentangle the multi-dimensional conformational dynamics of single proteins *in cellula* by combining long-term smFRET of cytosolic protein using an ALEX-based method[10,11] and three-channel tracking (Donor, FRET, acceptor)[12] and protein transfection.

Transfection of pre-labelled molecules allows for high degree of control of the number of molecules released and helps maintaining single molecule concentrations[13,14,15]. Additionally, it helps to observe newly introduced proteins while preserving the cell's native protein expression. While many transfection strategies have been established, transfection often creates background that introduces false FRET populations, in particular for proteins[14,16]. In addition, transfection efficiency of the protein is often not ideal, because the labelled protein is sometimes degraded or not homogeneously delivered. Therefore, different transfection strategies are employed based on the size, end destination within the cell and the stability of the molecules to be transfected. Generally the methods can be classified as physical, chemical or biological transfection methods[17,18,19]. Here we use two mechanistically different transfection strategies, a biological method using Streptolysin-O (pore-forming toxin)[20,21,22,23] and a physical method using microinjection[24,25,3], as both have the capability to introduce protein molecules with a higher molecular weight like Hsp90.

First we demonstrate the power of our method by comparing single-molecule conformations of pre-labelled Hsp90 *in vitro* and *in cellula*. This helps us to evaluate if *in vitro* conformatioal states reveal the ground truth of cellular behavior. For Hsp90 several *in vitro* single molecule studies show two distinct major conformational states, namely an open and a closed state[26,27,28], while such measurements were not possible in cells until now. On the other hand, bulk measurements in cells show that Hsp90 is involved in chaperoning function and is a target of multiple interactions and proteomic pathways[28,29,30,31], but the role of conformational states and dynamics in cells still remains elusive. As a first step towards monitoring the role of Hsp90's conformations in cellular processes, we use FRET-TTB to extract long-term FRET traces and stoichiometry information. We not only find differences between its behavior *in vitro* and *in cellula,* but also a dependency on the method of Hsp90 transfection into the cell, highlights the multi-dimensionality of protein dynamics in cells. In addition, we show a clear impact of cellular environment on standard dyes used in DNA or protein studies *in vitro*[2,32]. Altogether, presented here is a three-channel tracking for multi-dimensional protein dynamics in living cells enabling one to track diffusing species, to address the conformational dynamics and the spectrum of interactions that are present in living cells.

Results and Discussion:

Establishing *in cellula* long-term single molecule FRET measurements

Fluorescence measurements of proteins native to the cytoplasm have been largely done by confocal microscopy, resulting in short (millisecond) fluorescent bursts owing to free diffusion[3]. Long term fluorescence (seconds) has been achieved in cells on proteins localized to the membrane[1,33]. To obtain long term fluorescence for cytoplasmic proteins within various compartments, several challenges have to be overcome:

First, the freely diffusing proteins in the cytosol have to be slowed down, because to obtain sufficient signal to noise for tracking and distance determination (FRET) we need exposure times of around 100ms. With a diffusion constant of around D = 0.1 $\mu m^2/s$ for freely diffusing molecules in the cytosol, it is not possible to track molecules for several tens of seconds unless they are found in a non-diffusive state, i.e. bound to other molecules or trapped in organelles or vesicles. Therefore, here we slow down the pre-labelled Hsp90 (yeast Hsp90 with a cysteine at position 409 and 601, now simply referred to as Hsp90) by coupling it to a Neutravidin-anti-tubulin antibody complex (see Method 1 for details). This complex contains an anti-alpha tubulin antibody which helps to couple Hsp90 to microtubules within the cytoplasm. The complexing enabled partial immobilization or hindering of diffusion and helped to prolong tracking of the molecule over longer observation times. In addition, tracking the molecules continuously enables us to obtain diffusion and intensity parameters over time (Figure 1).

Second, TIRF-microscopy cannot be used to observe proteins in all compartments of the cell, as it is limited to regions close to the cover glass. Therefore we use a homebuilt HILO microscope (Fig.S2.1 for details on the setup), which largely spans the depth of HeLa cells as shown by Tokunaga, M., et al.[34]. In addition, we can change the depth at which the molecules can be observed within the cytoplasm independently from the excitation beam parameters. Since establishing FRET involves the need for dual-dye (donor and acceptor) measurements to get information on distance between the dyes[35,2], we need at least two colors. We have included two more colors, i.e. a total of four colors, in our HILO microscope to simultaneously observer FRET and localization in the cell (see Method 2). In addition, our HILO microscope enables alternating laser excitation (ALEX), which is required to obtain stoichiometry information and to clearly distinguish FRET states from non-FRET states (where the FRET between the donor and acceptor is hindered) of the molecule[10,36,37]. This sorting mechanism also helps to discriminate anticorrelated signals from acceptor or donor off-states and photobleaching effects, which otherwise might be misinterpreted as dynamics[38,2]. For the here investigated systems, a frame rate of 5.55fps with 70ms exposure was a good compromise between observing molecules on top of the background fluorescence level of the cell and obtaining long fluorescence traces.

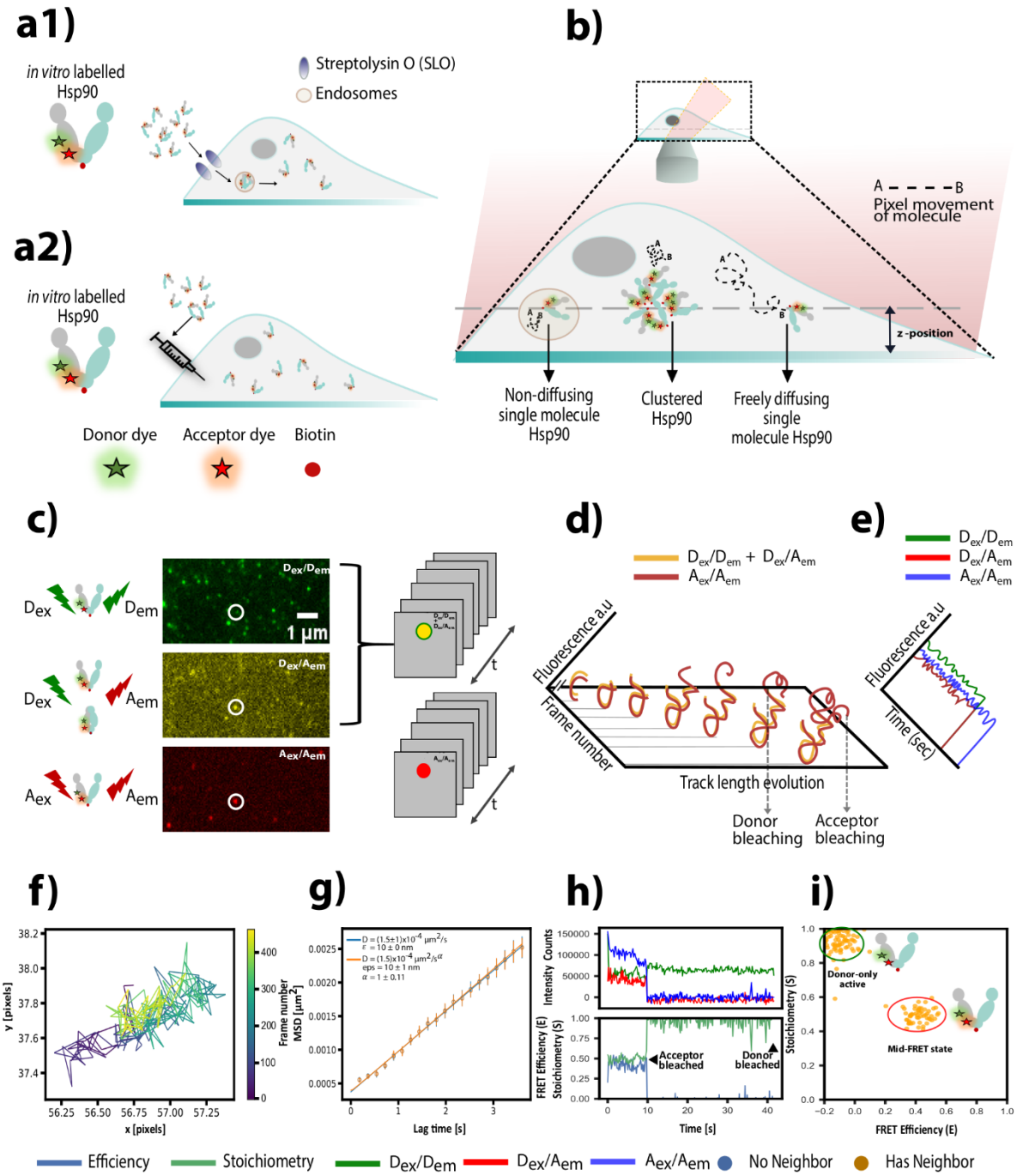

Fig.1: Schematic representation of strategies to obtain long-term tracking and smFRET signal from *in vitro* double labelled Hsp90 (LD555 and LD655) injected into the cytosol of cells. The process involves transfection of protein *via* a1) Streptolysin-O (SLO) toxin or a2) Microinjection. b) The transfected protein is then measured on the HILO setup using alternating laser excitation (ALEX). The enlarged panel shows the possibilities of protein complexes and diffusion profiles likely to be observed. c) Shows a sample image panel during the ALEX excitation-emission strategy (D_{ex}/D_{em}, D_{ex}/A_{em}, A_{ex}/A_{em}). d) Intensity signal from D_{ex}/D_{em}, D_{ex}/A_{em} channels are summed together and co-tracked with the A_{ex}/A_{em} channel, if one dye is bleached the other is still tracked. From this tracked trace we get the intensity curves. e) From the tracked intensity curves the summed channels are de-interleaved to get the individual intensities of the D_{ex}/D_{em}, D_{ex}/A_{em} and A_{ex}/A_{em} channels. Extracted results for a single molecule transfected *via* SLO are shown in f - i. f) The tracked coordinate map, G) diffusion plot, H) corrected intensity trace with bleaching steps for both dyes and i) corrected stoichiometry vs FRET efficiency plot (refer to Method 3 and 4 as well as Fig.S2.3 for correction factor and FRET efficiency calculation). In the E vs S plots we also indicate if the single molecule 'has neighbor' - another molecule is within the radius of background pixels of the current molecule being tracked, 'no neighbor' – no molecules are detected in the vicinity of the current tracked molecule. The diffusion plots give two diffusion coefficients. The blue fit is a linear fit assuming Brownian diffusion whereas the orange considers anomalous diffusion. ϵ gives the localization uncertainty, *eps* give the positional accuracy and α indicates the anomalous diffusion exponent (refer to Methods 5 for diffusion fit functions used).

Third, fluorescent proteins do not yield enough photons to be tracked and quantified over longer times. Therefore, synthetic fluorescent dyes, which yield up to a factor of ten more photons, have to be introduced. Establishing long term fluorescence with dyes on protein molecules can be facilitated by two methods, either dye-tagging proteins like HALO-tag, SUN-tag or SNAP-tag or by introducing *in vitro* labelled molecules via transfection methods. The tag-based methods pose a problem in controlled dual dye labelling of proteins. Additionally, one needs to control the cellular protein expression and calibrate dye concentrations for single molecule measurements. Further, the conformational dynamics of proteins might be hindered by the protein tag. Therefore, we used *in vitro* labelling of molecules, which has good control over the degree of labelling. In addition, dye parameters can be cross-verified *in vitro* before introducing into the cellular environment. This aids in studying labelled protein without compromising the cellular protein's expression level. To deliver the large about 180 kDa Hsp90 homodimer we tested two strategies: 1) Using a pore-forming toxin Streptolysin-O (Fig. 1A1), which transports proteins *via* pores across the plasma membrane into the cytosol[21]. 2) Microinjection via Femtojet II and InjectMan IV (Fig. 1A2). The double labelled Hsp90 (complexed or uncomplexed with Neutravidin and antibody) of 1 nM concentration of at least 70% degree of labelling for both dyes was injected into HeLa Cells. The latter method also allows to establish certainty in the number of labelled molecules introduced into the system.

Fourth, co-tracking of molecules in all three channels D_{ex}/D_{em}, D_{ex}/A_{em}, A_{ex}/A_{em} is necessary (Fig.1D), because the diffusing molecules may change their conformation between frames, which causes the intensity of the dyes to change and make tracking difficult. Here, D_{ex}/D_{em} is donor emission upon donor excitation, D_{ex}/A_{em} is acceptor emission upon donor excitation and A_{ex}/A_{em} is acceptor emission upon acceptor excitation. The signal from D_{ex}/D_{em}, D_{ex}/A_{em} channels were summed and tracked together with the corresponding co-localized signal from A_{ex}/A_{em} channel[12]. This helps to solve the problem of tracking the molecule during conformational changes (particularly in the case where $R_0<R$ for the labelled dye pair) as FRET efficiency changes and intensity changes in only one channel will not affect the tracking here. Labeled Hsp90 molecules with Lumidyne dyes LD555 (donor) and LD655 (acceptor) were introduced into HeLa cells *via* two different transfection methods 1) SLO and Microinjection (see Method 6, 7 and Supplementary note 1.2 for more details). All *in cellula* HILO measurements using SLO and microinjection are detailed in Methods 8-12. The single molecule intensity traces shown in Fig.1h indicate clear anti-correlated behaviour of donor-acceptor pairs and clear bleaching steps of both dyes demonstrate that the HILO-based observation of single molecule FRET *in cellula* performs as expected. Particularly, the additional A_{ex}/A_{em} signal helps to avoid misinterpretation of FRET dynamics as shown in (Fig.S2.4). For further analysis, tracks which are longer than 50 frames were screened manually. We discard tracks of less than 50 frames, because they contain limited information and do not allow for unambiguous determination of the following screening features (see Method 13 for tracking analysis and Fig.S2.5 for frame length-based trace classification). The screening incorporates selection of traces based on features of single molecules with donor and acceptor such as bleaching step analysis, anti-correlated behavior of donor-acceptor and stoichiometry (S) of FRET pair vs FRET efficiency (E). S vs E plots (Fig.1i) additionally add a clear way to understand the number of molecules which are present in a single trace helping to distinguish between clusters, the ratio of donors to acceptors and dye photophysics of the newly introduced labelled proteins inside cells. Finally, the diffusion parameters are important criteria as detailed in the next chapter.

Diffusion and intensity based differentiation of *in cellula* smFRET traces

Fig. 2 shows a comparison between the diffusion of *in cellula* tracked Hsp90 molecules observed when transfected with SLO vs Microinjection strategy (see Fig.S2.6 for the whole data set). SLO based transfection shows clear smFRET traces with single acceptor and donor bleaching steps (Fig.2A). This shows that HILO microscopy in the cytosol of living cells is able to detect smFRET for tens of seconds and therefore in principle to determine conformational dynamics. Predominantly non-diffusive,

stagnant states have been observed, for example the following values (Fig. 2d): $D=(1.8\pm1)x10^{-4}$ $\mu m^2/s^\alpha$ (α =1); $D=(1.4\pm1)x10^{-4}$ $\mu m^2/s^\alpha$ (α =1) and $D=(7.6)x10^{-5}$ $\mu m^2/s^\alpha$ (α =1.4). In contrast, microinjection of Hsp90 molecules often shows a much higher diffusion coefficient of e.g. $D=(3.6)x10^{-3}$ $\mu m^2/s^\alpha$ (α =1.5); $D=(5.5)x10^{-4}$ $\mu m^2/s^\alpha$ (α =1.3) and $D=(1.4\pm1)x10^{-3}$ $\mu m^2/s^\alpha$ (α =1.3) (Fig.2h). Altogether, microinjection resulted in molecules with a more diverse diffusive behavior from sub-diffusive α < =1 to super-diffusive α >1.3 states in comparison to the SLO transfected cells where the proteins were less mobile, which will be further investigated below. A previous study has shown that a similar sized Hsp90 variant (AaHsp90, a 160 kDa protein) possess a diffusion coefficient of $D = (2.7\pm0.3)x10$ $\mu m^2/s$ (ref.[39]) for free diffusion. This is consistent with our interpretation of hindered diffusion in our *in cellula* measurement. This does not exclude possible additional freely diffusing Hsp90 molecules, but such fast diffusing species would not be evaluated in our study as it generates poor trace quality and/or shorter tracks (we restrict analysis to tracks more than 50 frames for FRET efficiency evaluation).
Altogether, this indicates that SLO transfected Hsp90's is localized to specific compartments, where they are largely immobilized and can be detected very well. On the other hand, microinjected Hsp90's shows differently localized species, which differ in their diffusive behavior and their clustering behavior as further investigated in the following. Unfortunately, these intensity traces also show a higher degree of fluctuation without clear bleaching steps, in contrast to SLO transfection.

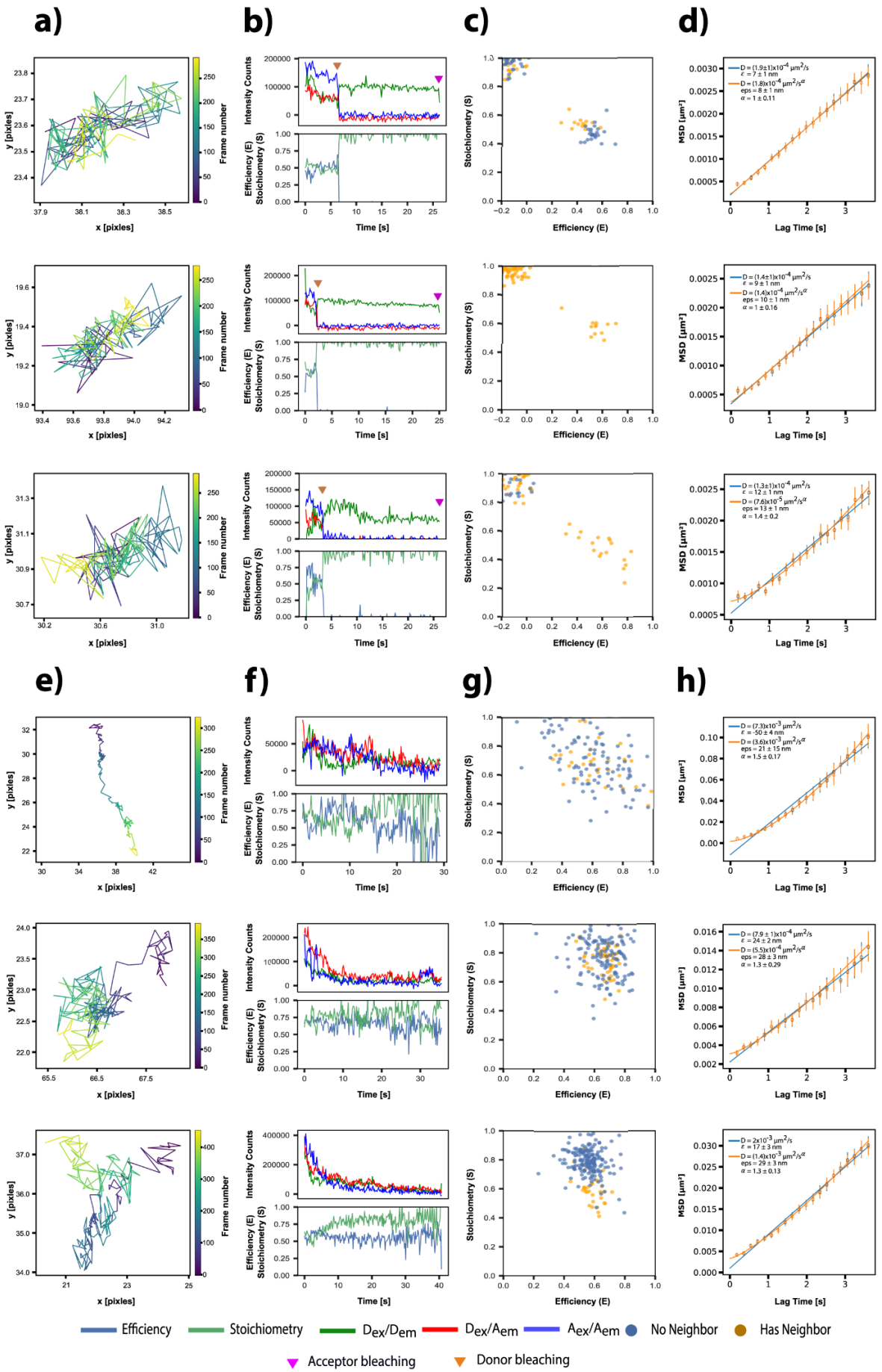
a)
b)
c)
d)
e)
f)
g)
h)
x [pixles]
y [pixles]
Frame number
Intensity Counts
Efficiency (E)
Stoichiometry (S)
Time [s]
MSD [µm²]
Lag Time [s]
Efficiency
Stoichiometry
Dex/Dem
Dex/Aem
Aex/Aem
No Neighbor
Has Neighbor
Acceptor bleaching
Donor bleaching

Fig.2: Examples of single molecule fluorescence data of double labelled Hsp90 with LD555 and LD655 *in cellula.* a to d) Transfection using SLO and e - h) transfection using microinjection. Corresponding tracked coordinate frames (A, E), intensity traces (b, f), stoichiometry vs FRET efficiency plots (c, g) and diffusion plots (d, h) are shown. In B, orange triangles show the acceptor bleaching steps and the pink triangles shows the donor bleaching steps. In plot c, a single FRET population in the mid-FRET range can be seen. The diffusion coefficient in d indicates static immobile non-diffusing molecules for SLO transfection. In f, the exponentially decaying traces indicate clustered Hsp90s. This is consistent with the higher stoichiometries in g. The diffusion plots in h show various diffusion behaviour with faster movements than the SLO transfected Hsp90s (refer to Fig.S2.5 and Fig.S.2.6 for a more detailed plots related to tracked frame lengths and whole dataset plots).

Improving single molecule FRET traces in the cytosol by slowing down diffusion and reducing clustering effects

In the above experiments we have obtained good smFRET data if Hsp90 was immobilized in a cellular compartment as e.g. for the SLO transfection. Fast moving Hsp90s, as they often occurred for microinjection, are likely free in the cytosol and difficult to quantify. One idea to obtain better smFRET data in the cytosol was to slow down the diffusion of biomolecules to allow for longer integration times. Therefore, we used and tested hindering the diffusion via neutravidin and anti-alpha tubulin antibodies (will be referred hereafter as neutravidin-antibody). Although, the slowdown of diffusion worked, the observed smFRET traces did not show the expected clear donor or acceptor bleaching step or the anticorrelated signal between them, which was observed in the SLO system.

To better understand smFRET in microinjected cells, we compared *in vitro* and *in cellula* (live cell) Hsp90 experiments with the same constructs on the same setup. Figs. 3:a,b show that the cellular environment has a big impact on labelled Hsp90's fluorescence and the signal-to-noise becomes worse. In order to find out, if this was caused by Hsp90's cellular environment or by changes in dye properties, we tested the same strategy on DNA with known positions of dyes (see Method 6) with ends sealed based on copper-based click chemistry (esDNA). We performed *in cellula* fixed cell experiments immediately after microinjection. For esDNA the FRET efficiency is only slightly reduced from the *in vitro* (see Fig. S2.7A2) to the *fixed cell* experiments (see Fig. 3c).

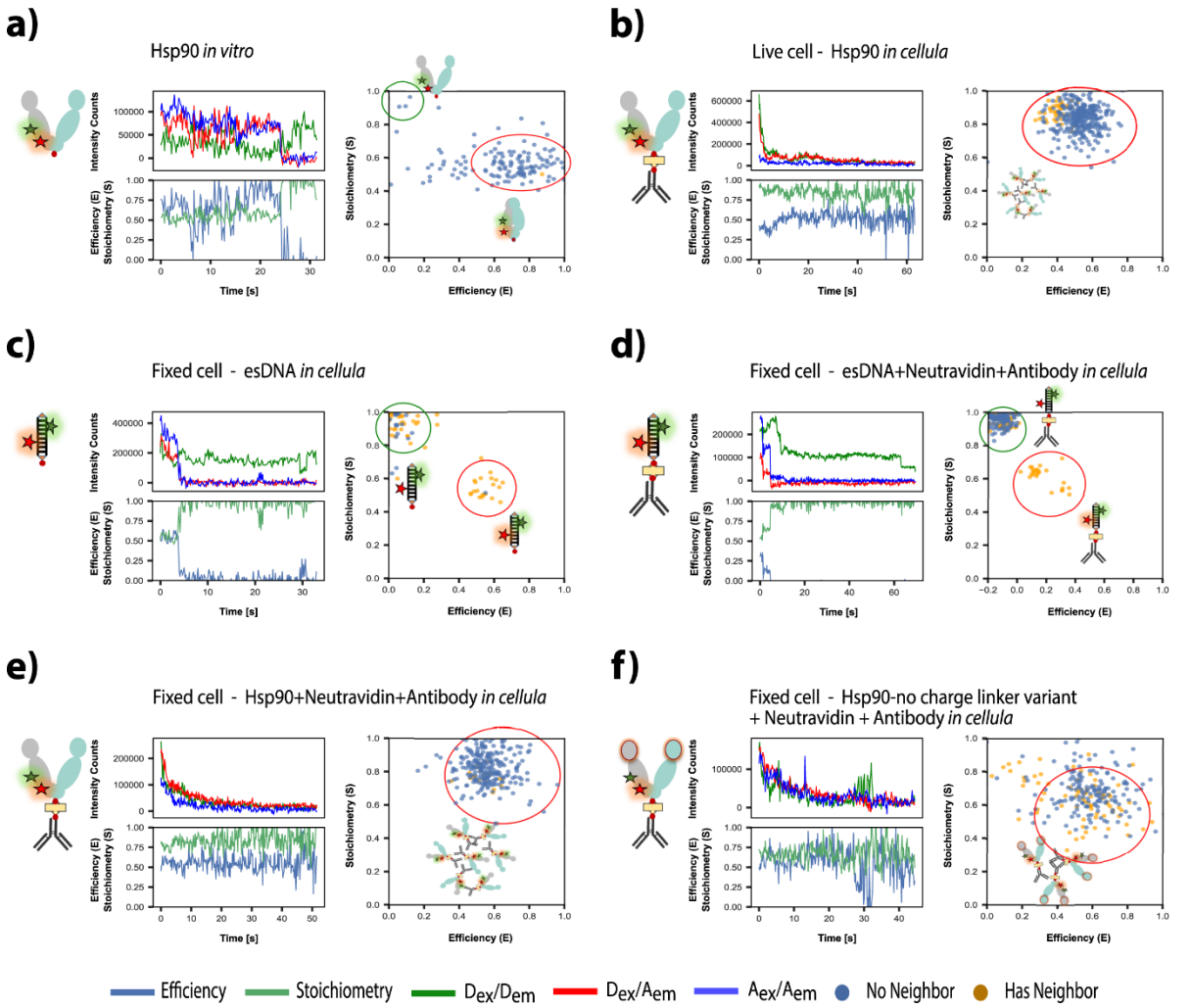

Fig.3: Shows experiments with Lumidyne dye labelled Hsp90, the labelling positions and dye parameters are given in (refer Supplementary note 1.2). A) Example single molecule traces of labelled Hsp90 *in vitro* immobilized on passivated glass slide with Biotin-Neutravidin conjugation measured in H1 buffer with pH 7.45. Leakage = 0.23, Direct excitation = 0.05, Excitation efficiency = 0.7, Detection efficiency = 1.0. B) Example single molecule traces of labelled Hsp90 conjugated with Neutravidin+Anti-tubulin antibody microinjected *in cellula*. C - F) Fixed cell experiments performed by microinjecting sample labelled with Lumidyne dye pair into live HeLa cells and then fixed with 4% Paraformaldehye (PFA) (refer Methods 7). Each sample set was measured separately and example traces are given for C) esDNA (without neutravidin+anti-tubulin antibody) *in cellula,* D) esDNA+Neutravidin+Anti-tubulin antibody measured *in cellula,* E) Hsp90+neutravidin+anti-tubulin antibody *in cellula,* F) Hsp90-no charge linker variant+Neutravidin+Anti-tubulin antibody measured *in cellula.*

Fig. 3d shows neutravidin-antibody complexed esDNA with clear bleaching steps with FRET efficiency at around E=0.3, i.e. a significantly shifted FRET efficiency, besides that we see another population at the higher stoichiometry population at S=0.8, indicating multiple donors in several cases. In both, uncomplexed and complexed esDNA, the signal intensity stays consistent at about 200000 counts to give good stoichiometric segregation between the FRET population and the donor-only parts. This shows that complexing with the neutravidin-antibody and the 'fixed cell environment' has some effect on the photophysics of the dye and the FRET efficiency of the molecule, making *in cellula* measurements even more important. Therefore, the instrumental calibration factors were determined *in cellula* by using injected esDNA labelled at known positions at fixed FRET distances with similar conditions of measurement as the protein measurements. The obtain correction factors are: leakage=0.25, ratio of excitation efficiency=0.7, direct excitation=0.1 and detection efficiency of dye pair=0.9 for the Lumidyne dyes (LD555+LD655), which was used in the above experiments.

Fig.3e shows fixed cell experiments of Hsp90 complexed to neutravidin-antibody with a population at E=0.5 and S=0.8. Most *in cellula* Hsp90 intensity traces show an exponential decay for Donor (D_{ex}/D_{em}) and FRET (D_{ex}/A_{em}) signal with small (unclear) bleaching steps and Stoichiometries around 0.8,

indicating strong quenching of the acceptor. Altogether, this is best explained by a clustering of labelled Hsp90 molecules. Our data further indicates that the clustering occurs irrespective of complexing with Neutravidin+antibody nor dye sticking as the esDNA shows no such population at S=0.8.

Motivated by the abundant data on cluster formation in living cells, which is often driven by intrinsically disordered regions, we created a Hsp90 construct, where the long disordered charged linker (containing mainly polar amino acid rich sequence) is replaced with a short GSS based linker sequence (referred to as Hsp90-no charge linker in the following) – similar to the construct for the crystal structure 2cg9 [40]. We injected this Hsp90-no charge linker variant into the cytoplasm of HeLa cells and observed the molecules after fixing the cells. Fig.3f shows that the Hsp90-no charged linker variant is different from the regular Hsp90 as to having a population at E=0.6 and S=0.65 and the intensity traces show a decrease in signal to ~100000 counts with intermittent donor signal. This indicates that the Hsp90-no charge linker variant does not cluster as strongly as the regular Hsp90, but does not completely abolish clustering. Together with further controls (see Supplementary note 1.3 – 1.6) our experiments show that many Hsp90s clusters immediately after injection into the cell, not before.

Discussion:

The developed bottom-up engineering approach is a controlled way to observe and understand the multi-dimensional dynamics of biomolecules in living cells. This includes diffusion, conformational changes and potentially protein interaction dynamics. This will be crucial to understand the function of proteins in different compartments of the cell. Here we demonstrated the power of this approach on the Hsp90 dimer.

With our home-built HILO setup we were able to observe and track single proteins several microns into the cell cytoplasm and other compartments. Two different transfection methods likely delivered the Hsp90 dimers into different cellular compartments and conformational states. SLO transfection showed slowly diffusing molecules with intermediate, mainly static FRET efficiency, likely representing Hsp90s delivered into endosomes or lysosomes. Microinjection showed relatively fast diffusing Hsp90 clusters. While the former method shows Hsp90 is likely to be loosely associated with other proteins, the latter forms distinct stable clusters which requires further investigation in the future.

The alternating laser excitation strategy was crucial to obtain signal information in three channels (D_{ex}/D_{em}, D_{ex}/A_{em}, A_{ex}/A_{em}) and enabled us to assess single molecule stoichiometry information apart from knowing photophysical properties of dyes *in cellula*. To further limit the mobility of the protein and to show the effect of the local environment on the protein, we bound the labelled molecules to neutravidin-anti-tubulin antibody which binds to microtubules in the cytoplasm. This slowed down molecules and allowed us to track intensity changes in all three channels, with the tracks ending only when both dyes bleach. From these tracks we could determine time resolved FRET efficiency, stoichiometry, diffusion parameters and cluster formation.

Altogether, we observe several different Hsp90 behaviors for the same double-labelled Hsp90 protein (Fig.4). Namely slowly-diffusing Hsp90s with diffusion constants around 10^{-4} $\mu m^2/s$ and faster diffusing Hsp90s around 10^{-3} $\mu m^2/s$. Traces from SLO transfected cells, show flat FRET intensities and clear bleaching steps. The slowly-diffusive state indicates entrapment, possibly within the early to late endosomes and vesicles due to release mechanism adopted by SLO toxin[20,21,22]. Then clusters of Hsp90 with exponentially decaying intensity traces from microinjected cells were observed. Finally, super and sub-diffusive states indicate molecular mobility hindrances coming from microtubules[41,42,43]. This is consistent with previous studies, which tracked larger proteins such as nucleoproteins and multi-protein complexes in *E. coli* and show sub-diffusive motion in the cytoplasm[44,45].

In addition, we have found that the clusters observed in microinjection experiments responds to a deletion of Hsp90's charged linker as seen from the drop in the signal of the intensity traces compared to Hsp90 with charged linker. As the charged linker is essential for the function of Hsp90 *in cellula* this

could further indicate that this clustering behavior observed *in cellula* is a relevant functional aspect of the protein[46,47,48]. Further proof with respect to response of Hsp90 to its immediate environment is illustrated by the fixed cell Hsp90 measurements. Hsp90 clusters do quickly form upon interaction with the changing environment after microinjection, as cells are fixed within ~3 minutes after injection. Another notable observation of comparing *in cellula* live cell to fixed cell traces was the decrease in fluctuations in intensity of the traces. This indicates that the live cell environment contributes further to intensity changes likely through interactions with other molecules. This can in the future be studied by introducing a third fluorescence color.

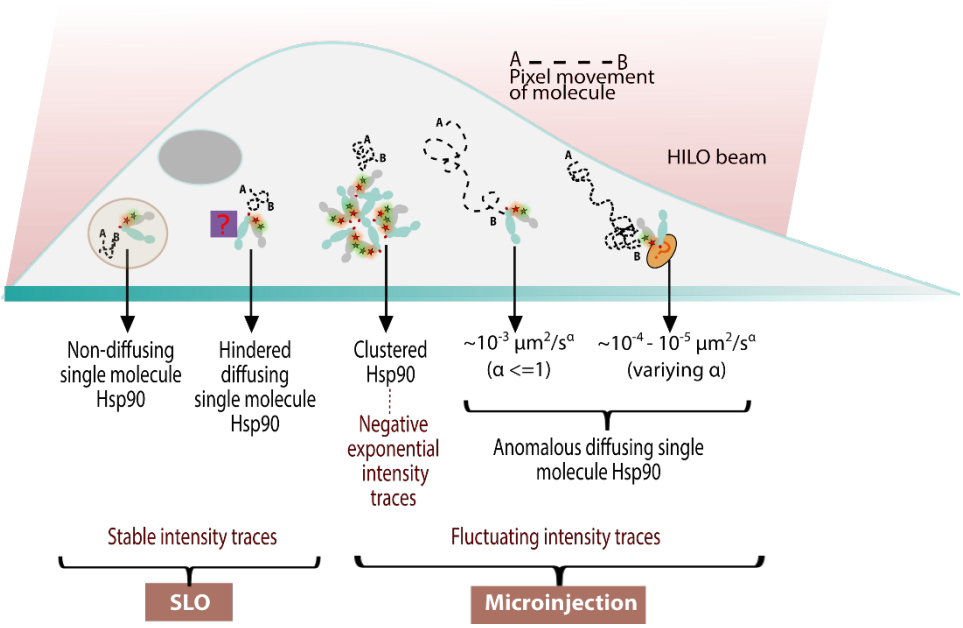

Fig.4: Summary of the type of molecules observed with the transfection strategies tested in this study (SLO and microinjection). Slowly-diffusing and hindered diffusing molecules were majorly observed in SLO transfected Hsp90. Different anomalous diffusion behaviour of Hsp90 molecules and their clustering were observed in microinjection. Altogether, our data shows that Hsp90 behaves differently in different locations or compartments of the cell. Such information can only be obtained if single molecule tracking and smFRET with ALEX are combined.

In conclusion we have shown a method based on single molecule FRET tracking and transfection of biomolecules (FRET-TTB) to investigate single biopolymers in living cells. FRET-TTB has enabled us to step into long-term fluorescent intensity analysis with smFRET and stoichiometric information, which was not possible before due to technical limitations and short observation times and short-lived fluorescent proteins. In addition, this method is not restricted to one region of the cell and is therefore a valuable tool to investigate protein plasticity and localization dependent function of proteins. Our study on Hsp90 already indicates that different regions within the cell significantly affect the mobility and conformation of Hsp90, as could be seen by the formation of protein clusters in one case. Our study can be further used to bridge the gap between *in vitro* and *in cellula* measurements to be able to test hypothesis proven *in vitro*. The precise control of the transfected proteins enables quantification of biomolecules' response to different cellular environments or compartments in an unprecedented way.

Acknowledgement

This work was supported by the Deutsche Forschungsgemeinschaft (DFG) under Germany's Excellence Strategy (CIBSS EXC-2189 Project ID 390939984) and the SFB1381 (Project ID 403222702) and by the European Research Council through ERC grant agreement no. 681891. We thank Dr. Bianca Hermann for her help in designing the yHsp90z_Avi_409C_601C-No Charge linker variant, to Veronica Frank for help in performing and analysis of smFRET-PIE confocal measurements, to Audrey Ayekoi for help in the FPS software theoretical FRET determination and AV simulations, to Jolanta Vorreiter and Michael Witt for their help in protein production of Hsp90 variants, to Marianne Birkle for help with the cell

cultures, to Prof. Dr. Ben Schuler for aiding us in running our initial tests of Hsp90 on their confocal injection setup, to Dr. Bismark Appiah for providing his expertise in handling the Femtojet II injector and micromanipulator for cell experiments, to Prof. Dr. Robert Grosse for eGFP-tagged tubulin protein.

Contributions

A.A., R.S. and T.H. designed research, A.A. performed experiments and data analysis, A.E. performed the SLO and microinjection volume experiments, P.W. performed the initial tests with SLO. L.S. and G.S. provided and optimized the three-channel tracking software with the help of A.A. A.A, T.H and C.L. designed and co-built the HILO setup. A.G.F and R.S. provided the initial seed culture and cell related expertise for this project. A.A. and T.H. wrote the manuscript with the help of all authors. All authors have given approval to the final version of the manuscript.

Methods:

1. **Ratiometric binding of molecules to neutravidin and anti-tubulin antibody:**

In microinjection experiments Hsp90 molecules were complexed with Neutravidin and Anti-tubulin antibody for the purpose of slowing down diffusion and partial immobilization *in cellula*. The procedure is as follows.

i) Mix Hsp90 or esDNA (labelled) with Neutravidin in ratios 1:1. An initial concentration of 2.5µM is used.
ii) Incubate for 1 hour shaking at 25° C.
iii) Wet 100 kDa spin filter (Merck) with **H1 buffer** (40 m*M* HEPES, 150 m*M* KCl, 10mM $MgCl_2$ pH 7.4), centrifuge 14000 rpm for 2 mins and throw away the filtrate (3x).
iv) Replace the filter into a new spin column.
v) Purify the Hsp90 (or esDNA) + Neutravidin mixture by centrifuging the sample with the spin column 14000 rpm, 10 mins.
vi) Invert the filter into a new spin column and collect the solution.
vii) Measure concentration* of the solution.
viii) Add 1.5x the antibody to the Hsp90 (or esDNA) + Neutravidin complex solution.
ix) Incubate the proteins at 4° C in a cold room for 48 hrs.
x) After 48 hours, wet 300 kDa spin filter with ATPase buffer. Follow steps 3 -4 (3x).
xi) Purify complex with 300 kDa spin filter, centrifuge 14000 rpm for 10 mins.
xii) Collect the retention fraction into a new spin tube.
xiii) Measure concentration.

* Note: The concentration of the complex is higher than the protein concentration used for binding. For ratiometric binding with the antibody, lowest dye concentration (LD555/LD655), obtained after Neutravidin+biomolecule filtration, is used instead of the total complex concentration. This ensures that after filtration more labelled molecules are obtained. Example calculation with a start concentration of 2.5 µM, 125 µl of Hsp90 results in 20.654 µM, 24.2 µl of Neutravidin+Hsp90 complex. This then is used for complexing with 3.75 µM, 66 µl of antibody, which then results in 2.62 µM, 20 µl of the whole complex (Hsp90 + Neutravidin + anti-tubulin antibody).

2. **Four-Color Single-molecule FRET HILO setup for live-cell microscopy:**

The four-color single-molecule FRET (smFRET) HILO microscopic setup is optimized specifically to study live cells. The layout of the setup is shown in Fig.S2.1. This setup is mainly designed for experiments dealing with dyes and fluorophores at emission wavelengths of 458nm (blue), 552nm (green), 638nm (Red) and 727nm (nearIR). All this is done while maintaining the maximal photon sensitivity for single-molecule (sm) experiments. These laser wavelengths give the flexibility to use the setup with

fluorescent proteins and chemical dyes according to the experiment. 458nm is needed to enable imaging of GFP, which is often used to locate the position within the sample.
To view the area of injection a 5x objective was positioned above the cell culture plate connected to scientific USB camera DCC1545M with a monochrome sensor (ThorLabs) (refer to supplementary Table 4.2 for more ThorCam parameters).
The donor-acceptor pairs used on this setup include Atto550-Atto647N and LD555-LD655. The 458nm laser is also used to identify the nucleus for the live cell experiments.

3. FRET efficiency calculation:

FRET efficiency and stoichiometry plots were calculated according to procedure outlined in Hellenkamp 2018[2]. Here we use the TIRF based calculation for the correction factor estimation and generation of FRET efficiency (E) vs Stoichiometry (S) plots.
The equations for the fully corrected traces are given as:

$$E = \frac{[(I_{Aem/Dex}) - \alpha(I_{Dem/Dex}) - \delta(I_{Aem/Aex})]}{\gamma[(I_{Dem/Dex})] + [(I_{Aem/Dex}) - \alpha(I_{Dem/Dex}) - \delta(I_{Aem/Aex})]}$$

$$S = \frac{\gamma[(I_{Dem/Dex})] + [(I_{Aem/Dex}) - \alpha(I_{Dem/Dex}) - \delta(I_{Aem/Aex})]}{\gamma[(I_{Dem/Dex})] + [(I_{Aem/Dex}) - \alpha(I_{Dem/Dex}) - \delta(I_{Aem/Aex})] + 1/\beta[(I_{Aem/Aex})]}$$

Where, $I_{Dem/Dex}$ is the intensity of donor emission upon donor excitation, $I_{Aex/Aem}$ is the intensity of acceptor emission upon acceptor excitation, $I_{Aem/Dex}$ is the intensity of acceptor emission upon donor excitation. All intensity traces were background corrected in the appropriate channels before applying correction factors. The traces were corrected for leakage of the donor into the acceptor channel (α), background offset, direct excitation of the acceptor upon donor excitation (δ), normalized excitation intensities and the cross-section of acceptor and donor (β) and the relative detection efficiency of the fluorophore pair (*γ)* as per Hellenkamp 2018[2]. The correction factors of *in vitro* traces were calculated separately in a home written IgorPro program as detailed before[49]. Then the estimated correction factors were applied to the SDT analysis program to be applied for all the traces to give the corrected FRET efficiency and Stoichiometry.

4. Correction factor estimation:

i. Channel Alignment:

For calculation of correction factors, *in vitro* datasets were analyzed using a home written IgorPro program. The donor and acceptor channel alignment were done using flurosphere beads selection mentioned in section 4.1 of Götz et al 2016[49]. For this study 1:100 dilution of bead solution in double distilled water (Flurospheres amine-modified, 0.2 µm, yellow-green fluorescent, Microspheres, Polysciences) was used. 20 µl of the bead solution was spread on a clean glass slide covered with a circular glass coverslip, after 10 minutes of incubation the bead solution was gently removed and 20 µl of water was covered again by coverslip and imaged. The laser is excited in continuous mode and the image of beads in both channels (Donor emission and Acceptor emission channels) is recorded. During imaging multiple fields of view are recorded for 100 frames. These movies are fed into the IgorPro program for channel registration correction. For correcting the inhomogeneity of laser excitation, a high concentration of dye labelled esDNA or protein is used (about 100 pM) to densely cover the surface. The same ROI used for channel alignment is measured with the same laser intensity. This is later used for flatfield correction in SDT.

ii. Correcting time traces:

The steps outlined as per section 4.2 of Götz t al 2016[49] was followed. The images used were of 2x2 binning with 2000 frames. Manually selected donor only, acceptor only, donor+acceptor traces were selected for further analysis. Then *in vitro* esDNA (ATTO dye correction factor and Lumidyne dye correction factor were separately done) measurement files were selected for analysis. The traces which showed clear bleaching steps with no dye photophysics (such as blinking) were manually selected. Once trace selection was done, donor-only and acceptor-only and FRET segments within the trace were marked. Then a Stoichiometry Vs Efficiency plot for the FRET

regions as well as the donor and acceptor regions were generated. The corresponding histograms for FRET populations were fitted with single exponential Gaussian fits as the esDNA used has only one FRET pair. The traces were corrected for α, δ, β, γ. The adjustments were made until the theoretical and the experimental FRET values were almost similar without compromising the leakage and direction excitation values. The same procedure was repeated for *in vitro* protein measurements and their corresponding correction factors calculated. Only slight deviation in correction factors was observed. Subsequently both the corrected traces and their respective E Vs S plots are generated. Refer to Fig.S2.7 for example uncorrected vs corrected trace of esDNA. In FigS2.7 A,C and B,D show the corrected traces for *in vitro* vs *in vivo* traces for esDNA and Hsp90 respectively with bleaching steps.

5. Diffusion fits:

The fit function for the Mean squared displacement (MSD) vs lag time graphs is:

$$(1)\quad MSD\text{tlag} = 4Dt_{app}^{\alpha} + 4\epsilon$$

Where, MSDtlag is the mean squared displacement for different lag times, D is the diffusion coefficient, t_{app} is the apparent time lag based on the movement of the particle within a fixed exposure time, α is the anomalous diffusion exponent (for particles not showing hindered diffusion this is 1), ϵ is the positional accuracy (uncertainty). The MSD vs lag time for the whole dataset or single molecules can be calculated by setting the ensemble parameter to True or False respectively. The standard error for the MSD is calculated based on standard deviation of square displacements divided by the number of samples. Pixel size of 160nm, 5.55fps, 70ms exposure time was used for calculations. Particle motion during exposure time was accounted for50. Along with the fits, the eps (positional accuracy) and fits corresponding to "anomalous" or "Brownian" diffusion are as well generated.

6. Labelled molecules:

i) End-sealed dsDNA (esDNA):

For standardization of the FRET in vitro and in *cellula*, the high-FRET dsDNA sequence (1-hi - T 19(C2) = D-strand, T 31(C2) = A-strand) pair was used as studied and described in Hellenkamp 2018[2]. One sample of dsDNA used was purchased from ATDBio and labelled with Atto550 and Atto647N. Another sample was labelled with LD555 and LD655. The ends of the dsDNA are sealed by click chemistry between 5' hexynyl group and 3' amino C7 labelled with azidohexanoic acid[51]. In the duplex the biotin dT is on the strand where the Atto647N is added. Changes were made to the carbon position at which the dyes were attached. The dyes were attached to thiamine group of C6 dT. Below is the sequence at which the dyes and the biotin groups were attached.

5'-**2**GAGCTGAAAGTGTCGAGT**5**TGTTTGAGTGTT**6**GTCTGG**3** -3'

Where,

2 = 5' hexynyl

3 = 3' amino C7 labelled with azidohexanoic acid

5 = amino C6 dT labelled with ATTO647N/LD655

6 = Biotin dT

5'-**2**CCAGACAAACACTCAAACAAACTCGACACT**5**TCAGCTC**3** -3'

Where,

2 = 5' hexynyl

3 = 3' amino C7 labelled with azidohexanoic acid

5 = Amino C2 dT labelled with ATTO550/LD555

Degree of labelling (DOL) of esDNA (ATTO550, ATTO647N) was found to be 116.288% and 95.235% respectively. DOL of esDNA (LD555, 6555) was found to be 126.314% and 90.705% respectively.

ii) yHsp90z_Avi_409C_601C:

Yeast Hsp90 protein was expressed and purified in our lab as per protocol mentioned in Supplementary method 3.1. The Hsp90 variant used for all the live cell and fixed cell experiments (unless otherwise mentioned) is the yHsp90z-Avi-409C_601C construct. This Hsp90 is a homodimer and contains a leucine zipper at the C-terminal end to enable monomer exchange of labelled protein with unlabeled protein. The 'Avi' in the name mentions that this protein expresses an Avi-tag which allows the protein to be biotinylated *in vivo* of the bacterial cell with the help of biotin ligase enzymes co-expressed in a pBirAcm (Avidity Nanomedicine, La Jolla, CA) plasmid[52]. The labelling positions are amino acids 409 and 601, which are in the Middle domain and C-terminal region, respectively (see Supplementary note 1.2 for labelling positions and AV calculations). At these positions the amino acids are replaced with cysteines so as to label with cysteine-maleimide chemistry. It is to be noted that the crystal structural of 2cg9 only resolves partially the C-terminal region.

Labelling was carried out separately with dye pairs ATTO550, ATTO647N and LD555, LD655 as mentioned in Supplementary method 3.2. The degree of labelling (DOL) for Hsp90 (ATTO550, ATTO647N) was 81% and 102.183% respectively. The DOL for Hsp90 (LD555, LD655) was found to be 62.071% and 65.251% respectively. Each labelled pair of Hsp90 was monomer exchanged with unlabeled yHsp90z-Avi-409C_601C protein in 1:1 ratio so as to obtain one dye pair per Hsp90 dimer. However due to the stochastic labelling strategy the ratio of the dye pairs generated will be more in the range of 1:2:1 for donor:donor+acceptor:acceptor. After labeling the protein was purified via size exclusion chromatography to remove excess dyes.

iii) yHsp90z_Avi_409C_601C_no-charge_linker variant:

The yHsp90z-Avi-409C_601C_no-charge_linker variant was synthesized to remove the full length charged linker and replaced with a short linker (LQHMASVD). The labelling strategy and purification is followed as given in Supplementary method 3.3 and the monomer exchange protocol is as mentioned in Supplementary method 3.4 The DOL of Hsp90 (LD555, LD655) was 55.6% and 120.823% respectively.

7. Fluorophores used in the study:

i) ATTO dyes: Fluorophores ATTO 550 and ATTO647N (ATTO Tec., Ltd) were used as a donor and acceptor pair which fits the setup multibandpass excitation and emission criteria.

ii) Lumidyne dyes: Fluorophores LD555 and LD655 (Lumidyne) were additionally used as a donor and acceptor pair which fits the setup multibandpass excitation and emission criteria.

8. Cell culture:

Different cell lines were tested to obtain low background for the dichroic used in the HILO setup. HeLa wildtype cells gave the lowest background in the orange and red channels used as donor and acceptor emission channels (refer Fig.S2.8 for details). Hence, HeLa wt cells were used in the study for all fixed and live cell experiments. Cells were cultured in Dulbecco's Modified Eagle's Medium (DMEM) without Phenol-Red (Thermo Fisher Scientific, Waltham, USA) supplemented with 10% Foetal Calf serum (FBS) (Gibco), 1% Glutamine (Sigma) and 1% penicillin-streptomycin (Sigma) so that a monolayer of loosely packed cells is achieved. Two hours before experiments they were switched to Opti-MEM I reduced serum medium (Thermo Fisher Scientific, Waltham, USA). The choice of using Opti-MEM I media for our imaging experiments were tested based on relative background testing yielding low counts and maintaining cell viability over 2 hrs (refer to Fig.S2.9 for details). Dulbecco's Phosphate buffer saline (DPBS) and Opti-MEM I were both separately sterile filtered twice with 0.5 µM syringe filters. Both were pre-heated to 37° C before starting the experiment. The cells are first washed twice with DPBS and then 2 ml of Opti-MEM I was added to the cells.

i) SLO Live cell experiments:

All experiments were performed with HeLa cells grown in 8 well glass bottom 170 µM thickness dish (µ Slide 8 Well ibidi®). For each replicate and each control one chamber was prepared. Per chamber 490 µl of DMEM medium (Gibco™) was inoculated with 10 µl of a confluent pre-culture of HeLa cells. 400 µl of the cell suspension were transferred to each chamber of an 8 well dish (µ Slide 8 Well ibidi®). HeLa cells were grown to 75% confluency at 37 °C for 1 day (40 - 45 h).

ii) Microinjection for fixed and live cell experiments:

The cultured HeLa cells were grown in a 35mm Ibidi dish with high wall, glass bottom 170 µM thickness, 500 grid (ibidi®). The cells were seeded two days before the experiment at 75% confluency such that a monolayer of loosely packed but connected cells are formed.

9. SLO transfection *in cellula* (HeLa cells):

Cells were grown to confluency at 37 °C in 8 well dishes for 1-2 days. Tyrode's buffer (140 mM NaCl, 5 mM KCl, 1mM MgCl2, 10 mM HEPES, 10 mM Glucose, pH 7.4) used for protein-dilution was degassed for 0.5 hr and Opti-MEM™ medium was filtered twice with 0.45 µm syringe filter (Merck Millipore millex) before starting the transfection procedure. The Opti-MEM™ medium was preheated at 37 °C. First the SLO stock solution (250x) was diluted to its working concentration (1x) with DPBS containing 1 mM $MgCl_2$. yHsp90z_409c_601c labelled with LD555 and LD655 was diluted with degassed Tyrode's buffer to a final concentration of 100 nM. Sample as well as control wells were washed with 400 µl DPBS containing 1 mM $MgCl_2$ and then 300 µl 1x SLO was added. After 10 min incubation of cells at 37 °C they were washed twice with DPBS+1 mM $MgCl_2$. Then 300 µl protein was added to the sample well and to negative control wells only Tyrode's buffer was added. The dish containing sample and negative controls were incubated for 5 min on ice. The wells were then washed thrice with Tyrode's buffer and 20 min incubation at 37 °C with recovery-medium (DMEM, 2 mM ATP, 10 % FBS; 300µl/well). Finally, the cells were washed twice with DPBS+1 mM $MgCl_2$ and the recovery medium replaced with 300 µl of Opti-MEM™. The cells were then imaged.

10. Microinjection *in cellula* (HeLa cells):

We used a fluorescence microscope (Axio Observer 3, Carl Zeiss Microscopy GmbH., Oberkochen) mounted with DIC module, Colibri 7 (excitation specific to UV (385nm), Blue-violet (430nm), Green (555nm), Yellow (590nm), Red (630nm), FarRed (735nm)), beam splitters (90HE (emission filters QBP 425/30+514/30+ 592/30+709/100), 110 HE (QBP 425/30+524/51+634/38+785/38), BS 652 (Reflection 350-644nm>=98%, Transmission 660-950nm>=93%), filter wheel (692/40 Brightline HC, 809/81 Brightline HC) and Axiocam 702 mono camera. For injection a 20x Zeiss air objective was used. The injection system used is Femtojet 4i (Eppendorf) with a micromanipulator InjectMan 4 (Eppendorf). The injection needles Femtotip II (Eppendorf) were used for injection. The needles were filled with the protein sample using microcapillaries (Eppendorf). Then the needles were fitted into the microinjector nozzle. The angle of the microinjector was maintained at 45˚ (refer to Supplementary Table 5.3 for other parameters)

Injections were made in HeLa Cell wildtype. The cells were washed with pre-heated DPBS 1 ml twice and then 2 ml of Opti-MEM was added and set in the incubator at 37° C. All protein samples, esDNA and negative controls for injections were diluted in H1 buffer containing (40 mM HEPES, 150 mM KCl, 10 mM MgCl2 pH 7.4). Injections were made with Injection Pressure=300 hPa, Time=0.5sec, compensation Pressure = 30 hPa aimed at the cytosol of a monolayer cell culture (refer Supplementary note 1.4 further details). A grid square is selected and the image of the cells before injection is acquired in all channels. Cells in the specified grid square were injected and imaged after injection. The cells were then washed twice with DPBS and then supplemented with Opti-MEM and incubated for 1 hour at the HILO setup stage holder which is pre-set at 25° C. Then the cells were imaged. Once image acquisition is completed, the cell area which was injected was checked again and image are recorded

in the fluorescence microscope to check the health of the injected cells (refer to Supplementary note 1.4. D and E for positive and negative control test of microinjection respectively).

11. Sample preparation for HILO measurements:

i) *in vitro*:

i. Pre-Cleaning:

1. Take 10 coverslips (170µm, ROTH GmbH) in a coverslip rack and place them in a glass beaker or glass rectangular jars.
2. Fill the jar with fresh Hellmanex® III (Hellma Analytics) (1-2x) for 20 minutes.
3. Then wash the coverslips with ddH_2O.
4. Fill the jar with fresh ddH_2O and sonicate again for 20 minutes.
5. Discard the water, fill in 50/50 Isopropanol/ ddH_2O or 50/50 Ethanol/ ddH_2O and sonicate for 20 minutes.
6. Repeat steps 3 and 4.

ii. RCA-Cleaning:

1. Mix ddH_2O, Ammonia (30%) and Hydrogen peroxide (30%) in a ratio of 5:1:1 for a volume of 200 ml and fill the glass jar.
2. Place the coverslips rack in the mixture glass holder.
3. Heat the coverslips containing the mixture in an oven at 60°C for 2hours.
4. Discard the RCA solution safely. Wash the coverslips thoroughly with ddH_2O.

iii. Passivation:

1. Wear disposable gloves to handle the slides.
2. Place two glass or disposable pipettes on top of wet paper tissues that are laid out flat.
3. The glass coverslips are to be placed onto them after aminosilanization.

iv. Amino-silanization:

1. Submerse coverslips racks onto jar containing acetone (~200ml) for 10 min.
2. Incubate in 600 µL APTES (or Vectabond) diluted in 120 mL acetone for 10 min
3. Sonicate the jar containing slides and mixture for 1 minute.
4. Continue incubation further for 10 minutes.
5. Submerse the slide containing rack in a fresh acetone filled jar for 5 minutes.
6. Blow dry each slide with Nitrogen or Argon gas. Then place the slides in fresh dry coverslip rack.

v. PEGylation:

1. Place half the coverslips onto the pipettes set out in passivation (step iii).
2. Pipette 80 µl of PEG solution (600 µL 100mM $NaHCO_3$ pH 7.5, 80 mg methoxy-PEG-NHS (5 kDa), 3 mg biotin-PEG-NHS (3 kDa) (Rapp Polymers)) onto them, 80 µL per glass slide.
3. Create 'sandwiches': put a second coverslip on top of the first one.
4. Keep 'sandwiches' overnight at 4° C.
5. Wash off unbound PEG solution under running ddH_2O.
6. Dry coverslips with nitrogen or argon gas. Store them dark and dry.

vi. Imaging:

1. Prepare the PEGylated coverslip for imaging by attaching pre-made block resin (with 0.5 cm holes cut out for solution addition) using epoxy glue, make sure the glue does not cover the hole area when pressed.
2. Add 500 µl of Neutravidin to the glass coverslip (25 mg/mL in H1 buffer - 40 mM HEPES, 150 mM KCl, 10mM $MgCl_2$ pH 7.4) and incubate for 10 min.
3. Filter GODCAT buffer (0.1 µM Glucose Oxidase (from Aspergillus Niger), 1.5 µM Catalase (Bovine Albumin), 5.56 mM Glucose (Sigma-Aldrich), 2mM Trolox (Sigma-Aldrich) dissolved in Tris buffer (5 mM TRIS, 5 mM NaCl, 20 mM $MgCl_2$, pH 7.5 (all chemicals from Sigma-Aldrich)

(for esDNA) and H1 buffer for Hsp90 with 0.45 µm sterile syringe filter (Merck Millipore Millex).

4. Wash off the Neutravidin solution in the wells.
5. Add biotinylated labelled esDNA 10 pM of (500 µl) (prepared in Tris Buffer) or 30 pM of labelled Hsp90 (500 µl) (prepared in H1 Buffer) and Incubate for 5 - 10 mins.
6. Wash the wells with 500 µl of Tris buffer (for esDNA) or H1 (for Hsp90) (Gently pipette out).
7. Add fresh GODCAT buffer 500 µl such that the surface is covered.
8. Wait for 5 min and wells are ready for imaging.

ii) *in cellula*:

The labelled esDNA or Hsp90 mentioned in Method 6 (complexed with Neutravidin-anti-tubulin antibody) was injected into the HeLa cells as per the injection procedure mentioned in Method 10. The complexed purified esDNA of 1nM is prepared in a vial with degassed buffer which is double filtered. The injection needle is filled with 5 µl of 1nM esDNA complex and fitted to the injector nozzle. Before injection, the cell area to be injected is imaged in the DIC, Green (555nm), Red(630nm) emission channels of the fluorescence microscope to check for any leakage or fluorescence abnormalities. The grid number on the ibidi dish noted. The cells are then washed twice with DPBS 1ml (pre-warmed at 37 ˚C) followed by addition of Opti-MEM 2 ml. The cells are allowed to incubate at 25˚ C for 1 hour for the antibody to bind. Then measurements are made as per Method 12.

iii) Fixed cells:

The labelled esDNA or Hsp90 was complexed with Neutravidin-anti-tubulin antibody as mentioned in Method 1. The complexed purified esDNA of 1nM is prepared in a vial with degassed buffer which is double filtered. Injection needle is filled with 5 µl of 1nM esDNA complex and fitted to the injector nozzle. Before injection, the cell area to be injected is imaged in the DIC, Green (555nm), Red(630nm) emission channels of the fluorescence microscope to check for any leakage or fluorescence abnormalities. The injections procedure is followed as mentioned in section 3. The grid number on the ibidi dish is noted. The cells are then washed twice with DPBS 1ml (pre-warmed at 37 ˚C) followed by addition of 500 µl of Paraformaldehyde (PFA). The dish is incubated for 20 mins in dark at room temperature. Then the PFA is washed twice with in DPBS and 2ml of Opti-MEM was added. Then measurements are made as per Method 12.

12. HILO measurements:

The measurement parameters used for esDNA standards or Hsp90 protein were the same. In both cases the setup was maintained at 25° C. A diffused light source is pointed at the stage to illuminate the cell area. To view the injected cell area, a light microscope module with the CMOS camera (DCC1545M, ThorLabs) positioned above the stage is brought into focus until the view of the cells appear on the ThorCam software (ThorLabs). It is important to position the light microscope module directly above the objective lens, such that the center of the field of view of the light microscope image acquired is aligned with the objective lens. The dishes for *in vitro* experiment or injected cells were set on the pre-set holder. To get a good image of the Ibidi dish grids the ThorCam position was set and the software parameters adjusted as per Supplementary Table 4.3. Once the position of the grid was clearly visible, the 100x objective lens is brought into focus such that it is directly in the area of injected cells. This is done by using the 458nm laser to guide the center of the beam position towards the injected grid square.

The two EMCCD cameras Xion Ultra 987 (Oxford Instruments) sensors are cooled to -95° C with a water cooler set at 17° C. Camera settings are optimized for single-molecule recording (3.3 µs vertical shift speed, normal vertical clock voltage, 17 MHz, 16-bit horizontal read out, preamplification gain 3, gain

of electron multiplier 100, ROI defined for 182x179 pixel, 2x2 binning). As both cameras simultaneously record signal, electronic shutters are used (ThorLabs) and set to manual open mode ready to record signal. A triggering module (LabView) with a custom-written software triggers both the excitation of the lasers with the camera. The triggering module also incorporate the movement of the xy-micrometer (MadCityLabs)stage. We start acquiring the image of the cells in video mode to set the depth of height using a z-piezo (MadCityLabs) exciting the dyes with 553nm and 637nm lasers in ALEX mode. Images were recorded with an exposure time set to 70ms for both lasers with a camera read out time of 20ms, EM gain 300 and 2000 frames. Analysis was done using our SDT software. Molecules were selected based on their fluorescence in the donor, acceptor channels. Donor-only, acceptor-only molecules were selected by looking for single bleaching steps in the respective channels. FRET traces were selected by the anti-correlation behavior after acceptor bleaching. Stoichiometry vs FRET efficiency plots are generated and the corresponding correction factors for donor bleed-through, acceptor direct excitation and detection efficiency of the dyes were calculated (see Method 3 and 4).

13. Tracking and smFRET analysis of moving particles:

The smFRET analysis software[53] previously used to evaluate single-molecule force sensors in the immunological synapse[12] was adapted. Information about routines and their parameters can be found in the respective Python docstrings, which are part of the software. Additionally, an in-depth tutorial has been published[54]. Different sets of parameters were used to analyze esDNA and Hsp90 data as outlined in the below sections. A table of parameters can be found in Supplementary Table 4.3.

i) Loading datasets:

The data directory location, the type of measurement, the donor and acceptor image file locations, image files (donor and acceptor channel) used for channel registrations and flatfield corrections are specified separately in the Tracking Jupyter notebooks part of the smFRET analysis software package. Please refer to the tutorial for more details. The ALEX scheme of 'da' indicating donor excitation first followed by acceptor excitation is specified. A single-molecule localization algorithm based on finding fluorescent features' centers of mass[55] as implemented in the sdt-python package[56] was chosen due to its robustness in dealing with difficult signal-to-noise ratios.

ii) Channel registration:

The movies recorded for bead calibration are used in the channel alignment and correction factor calculations respectively. The procedure for the sample preparation and recording the movies are outlined in Method 4i. In the Tracking Jupyter notebook by executing the tr.set_registration_loc_opts (), the window for channel registration parameters is viewed. 'Grocker-Grier' algorithm was selected for all our analysis. The radius of particle to be localized was set to 2 pixels. Both these parameters are commonly set for donor and acceptor channels. The donor signal intensity and mass thresholds were set to 1000 and 1000, whereas the acceptor signal intensity and mass threshold were set to 500 and 1000 respectively. Once above parameters are set for the donor and acceptor channels, move to a frame in the movie where well distributed single molecule beads are found and click through 10 frames to ensure the adequacy of the chosen options. Following this, the registration calculation (tr.calc_registration()) was done.

iii) Single-molecule Tracking:

i. For localization and tracking cell movies are used. Thresholding is applied for intensity in both donor and acceptor channel for channel alignment and localization of molecules. Channel alignment with registration difference of <0.3 pixel was considered to be good alignment. Once channel alignment is done next step is to track the molecules in the cell movies.

ii. Trackpy[56] was used as a single-molecule tracking algorithm. For determination of single-molecule fluorescence intensities, sdt-python's `brightness.from_raw_image` function was employed. Parameters used for different samples are listed below. The tr.set_loc_opts() displays the parameters needed to be set for intensity thresholds, tr.locate() runs the localization module, tr.track() runs the tracking module, tr.make_flatfield() reconstructs excitation laser profiles for flatfield correction and finally tr.save() is executed to save the tracked files.
iii. **smFRET of tracked esDNA:** The radius of integration is set to 2. Signal intensity threshold is set at 1000, mass threshold is set at 15000 for donor and 500 and 10000 for acceptor. The tracking parameters are set as follows: co-localization distance: 2.0, excitation sequence: da, interpolation: true. Linking of particles tracked between frames are set as follows: search range: 2, memory: 20, minimum length of each tracking was set at 20, neighbor radius: 2, brightness parameters are set as follows: radius: 2, background frame: 3, background estimator: mean, mask: circle.
iv. **smFRET of tracked yHsp90:** The radius of integration is set to 2. Signal intensity threshold is set at 1000, mass threshold is set at 20000 for donor and 500 and 15000 for acceptor. The tracking parameters are set as follows: co-localization distance: 2.0, excitation sequence: da, interpolation: true. Linking of particles tracked between frames are set as follows: search range: 2, memory: 20, minimum length of each tracking was set at 20, neighbor radius: 2, brightness parameters are set as follows: radius: 2, background frame: 3, background estimator: mean, mask: circle.
v. For **flatfield correction**, multiple field of view of densely labeled samples were averaged separately using maximum sum projection (imagJ plugin) to generate a summed image for donor and acceptor channels separately. These images are then fed to the tr.make_flatfield() module and smoothed using a Gaussian filter (σ = 10 pixels). The camera baseline (200 counts per pixel) was subtracted.
vi. The tracked files are saved. The following files are generated tracking-split-v013.yaml, tracking-split-v013.h5, tracking-split-v013.flat_donor.npz, tracking-split-v013.flat_acceptor.npz and tracking-split-v013.cell_img.npz.

iv) Single molecule track selection:

i. The inspector GUI (see Fig.S2.10) is used for selecting individual particles with the right stoichiometry and intensity. By running the python "-m smfret_analysis.inspector_gui" command on the command line prompt in anaconda the GUI can be viewed.
ii. Molecules having > 50 and <1000 frames of tracking length are selected (unless otherwise specifically doing <50 frame analysis for controls).
iii. Each molecule is evaluated manually and marked as selected or discarded. The marking is then saved. Molecules having donor only, acceptor only, or donor+acceptor are selected. The data is saved.

v) Correction factor estimation and calibration of selected traces:

The preparation of samples for channel registration and correction factor estimation are given in Method 4. The correction factor estimation was done using IgorPro v6.37. Refer github (https://gitlab.physchem.uni-freiburg.de/ak.hugel/TIRFrepo.git) for full TIRF traces analysis modules. The iniTIRF.ipf, addon_SEcorr.ipf modules are loaded and compiled in Igor Pro. Compiling the iniTIRF.ipf module opens the setup profile for the ALEX scheme that is operated. PW:ex g: det g+r is used for channel registration and PW alex: ex g/r : det g+r/r is used for ALEX measurements used for calibration purposes. Since we have two detectors the donor and acceptor channel movies are combined together and fed to the load film option.

i. **Channel registration:** Under tools, smFRET new option is chosen, then Analysis GUI is selected. In the Analysis GUI the donor and acceptor movies for channel is loaded. The sum Frames=5, Sum pixels = 2, Exclude pixels = 3 is maintained for all analysis. For each intensity trace is extracted by binned pixels of 2x2 around the central highest intensity spot and the continuation of the trace is based on the sum frames function and the background pixel is the 'exclude pixels' specified around the summed pixels[57]. Then 'AutoSave off' is selected. Following this, the Calib panel is selected. The Calib panel opens the window for bead selection. minPeakHeight: 100, GaussFitArea: 2, SigmaLimit: 2 are set. Then Auto Calib is pressed. Once the beads through all the frames are selected. We can press 'fit Calib' option. This generates the coefficients for all channels (coefxgnr, coefygnr, coefxrng, coefyrng) in the coef folder and gives the graphFitAll and the GraphFitDiff plots. If the alignment is good, the difference in pixel is <0.3. Then we can load the dark noise and excitation profile images by running the get_iMap().

ii. **Correction factor calculations:** The *in vitro* esDNA or *in vitro* Hsp90 movies used for correction factor estimation is then loaded to the Analysis GUI. Estimation of correction factor for alex traces is based on Lee et al., 2005[58]. Once set, the 'Find traces' option helps to populate the traces observed within the movies. Selection of time traces is as per described in Wortmann et al, 2017[57]. Each trace is selected by pressing the 'use it' option and saved for later analysis. The intensity traces are corrected for dark current of the EMCCD and the background fluorescence. Detailed steps on how to correct each trace is given in the addon_SEcorr.ipf file. The corrected *in vitro* measured esDNA and Hsp90 are given in Fig.S2.3.

iii. **Correction factor for *in vitro* esDNA:** Estimated correction factors are leakage: 0.25, direct excitation: 0.1, ratio of excitation efficiency: 0.6793, ratio of detection efficiency of dye pair (LD555+LD655): 0.8645.

iv. **Correction factor for *in vitro* Hsp90:** Estimated correction factors are leakage: 0.23, direct excitation: 0.05, ratio of excitation efficiency: 0.7, ratio of detection efficiency of dye pair (LD555+LD655): 1.

v. **Cross-verification of correction for *in cellula* traces:** *in cellula* traces showing FRET with clear bleaching steps and donor anti-correlation behavior after acceptor bleaching were selected and corrected with the same correction factors as mentioned in 3 and 4. The drop in leakage and The total intensity counts after correction factors applied were ensured (refer Fig.S2.7 for example uncorrected vs corrected traces). Following this correcting the traces in sdt software Data analysis section was done.

vi) Data analysis:

i. The updated analysis.ipynb file (with selected functions from the main 02. Analysis.ipynb file is uploaded in the Program folder) is opened and the tracked data is loaded by constructing an smfret_analysis.Analyzer Python object.

ii. Flatfield correction is applied using the ana.flatfield_correction() method. Then the calculation of the apparent FRET values is done by executing ana.calc_fret_values(a_mass_interp="next", skip_neighbors=False).

iii. Following this the correction factors pre-calculated from 5 were set and applied to sdt (ana.set_leakage(), ana.set_direct_excitation(), ana.set_detection_eff(), ana.set_excitation_eff()).

iv. Then the correction is applied to all traces using ana.fret_correction(). Following this the ana.save() is executed with data is saved saved as "Analysis_Full_corrected" if correction factors at step3 is applied or as "Analysis_Full_uncorrected" if step 3 is not executed. The saved data is saved as .h5 file format.

v. For plotting the E Vs S histogram, single molecule traces E_vs_S_Plot_total.ipynb (with selected functions utilizing the Plotter, Analyzer classes from the smfret_analysis package) is

executed, the appropriate corrected/uncorrected analysis data saved was loaded. Plots specific for 1. Uncorrected molecules, 2. Corrected molecules, 3. Diffusion data are plotted. Then only the molecules manually selected are plotted into the E Vs S plot and their respected histogram.

vii) Diffusion analysis:

i. The selection of molecules or traces was done as in section 3 of the E_vs_S_Plot_total.ipynb.
ii. The saved traces are then evaluated for diffusion coefficient in the E vs S plot_total script.
iii. To generate fits for Brownian and anomalous diffusion, parameters such as the frame rate = 5.55, pixel size = 0.16 µm, exposure time = 0.070 s, initial alpha = 0.34, MSD fit ='Anomalous' (defaults to Brownian if unspecified) , lag time was set to infinity (defaults to 100) are specified for the tracked movies.
iv. The fit for the mean squared displacement vs lag time gives the diffusion coefficient D, the eps value and alpha. The fits are explained in Method 5.
v. The mean squared displacement in the Z-direction based on the depth of view for the 2D diffusing molecules is calculated in supplementary note 1.6.

References:

1. Asher, W. B. *et al.* Single-molecule FRET imaging of GPCR dimers in living cells. *Nat. Methods* **18**, 397–405 (2021).
2. Hellenkamp, B. *et al.* Precision and accuracy of single-molecule FRET measurements—a multi-laboratory benchmark study. *Nat. Methods* **15**, 669–676 (2018).
3. König, I. *et al.* Single-molecule spectroscopy of protein conformational dynamics in live eukaryotic cells. *Nat. Methods* **12**, 773–779 (2015).
4. Sakon, J. J. & Weninger, K. R. Detecting the conformation of individual proteins in live cells. *Nat. Methods* **7**, 203–205 (2010).
5. Sako, Y., Minoguchi, S. & Yanagida, T. *Single-molecule imaging of EGFR signalling on the surface of living cells*. *NATURE CELL BIOLOGY* **2**, (2000).
6. Murakoshi, H. *et al.* Single-molecule imaging analysis of Ras activation in living cells. *Proc. Natl. Acad. Sci. U. S. A.* **101**, 7317–7322 (2004).
7. Okamoto, K., Hibino, K. & Sako, Y. In-cell single-molecule FRET measurements reveal three conformational state changes in RAF protein. *Biochim. Biophys. Acta - Gen. Subj.* **1864**, 129358 (2020).
8. Lakowicz, J. R., Szmacinski, H., Nowaczyk, K., Berndt, K. W. & Johnson, M. Fluorescence lifetime imaging. *Anal. Biochem.* **202**, 316–330 (1992).
9. Suhling, K., French, P. M. W. & Phillips, D. Time-resolved fluorescence microscopy. *Photochem. Photobiol. Sci.* **4**, 13–22 (2005).
10. Kapanidis, A. N. *et al.* Fluorescence-aided molecule sorting: Analysis of structure and interactions by alternating-laser excitation of single molecules. *Proc. Natl. Acad. Sci. U. S. A.* **101**, 8936–8941 (2004).
11. Kapanidis, A. N. *et al.* Alternating-Laser Excitation of Single Molecules. *Acc. Chem. Res.* **38**, 523–533 (2005).
12. Göhring, J. *et al.* Temporal analysis of T-cell receptor-imposed forces via quantitative single molecule FRET measurements. *Nat. Commun.* **12**, 1–14 (2021).
13. Nelson, E. M., Kurz, V., Shim, J., Timp, W. & Timp, G. Using a nanopore for single molecule detection and single cell transfection. *Analyst* **137**, 3020–3027 (2012).
14. Fu, A., Tang, R., Hardie, J., Farkas, M. E. & Rotello, V. M. Promises and Pitfalls of Intracellular Delivery of Proteins. *Bioconjug. Chem.* **25**, 1602–1608 (2014).
15. Yu, J. Single-Molecule Studies in Live Cells. *Annu. Rev. Phys. Chem.* **67**, 565–585 (2016).

16. Verdurmen, W. P. R., Mazlami, M. & Plückthun, A. A quantitative comparison of cytosolic delivery via different protein uptake systems. *Sci. Reports 2017 71* **7**, 1–13 (2017).
17. Kim, T. K. & Eberwine, J. H. Mammalian cell transfection: the present and the future. *Anal. Bioanal. Chem.* **397**, 3173–3178 (2010).
18. Fus-Kujawa, A. *et al.* An Overview of Methods and Tools for Transfection of Eukaryotic Cells in vitro. *Front. Bioeng. Biotechnolology* **9**, 634 (2021).
19. Ebrahimi, S. B., Samanta, D., Kusmierz, C. D. & Mirkin, C. A. Protein transfection via spherical nucleic acids. *Nat. Protoc.* **17**, 327–357 (2022).
20. Walev, I. *et al.* Delivery of proteins into living cells by reversible membrane permeabilization with streptolysin-O. *Proc. Natl. Acad. Sci. U. S. A.* **98**, 3185–3190 (2001).
21. Corrotte, M., Fernandes, M. C., Tam, C. & Andrews, N. W. Toxin Pores Endocytosed During Plasma Membrane Repair Traffic into the Lumen of MVBs for Degradation. *Traffic* **13**, 483–494 (2012).
22. Stewart, S. E. *et al.* Assembly of streptolysin O pores assessed by quartz crystal microbalance and atomic force microscopy provides evidence for the formation of anchored but incomplete oligomers. *Biochim. Biophys. Acta - Biomembr.* **1848**, 115–126 (2015).
23. Teng, K. W. *et al.* Labeling proteins inside living cells using external fluorophores for microscopy. *Elife* **5**, 1–13 (2016).
24. Shimizu, N., Kamezaki, F. & Shigematsu, S. Tracking of microinjected DNA in live cells reveals the intracellular behavior and elimination of extrachromosomal genetic material. *Nucleic Acids Res.* **33**, 6296–6307 (2005).
25. Wegmann, S. *et al.* Tau protein liquid–liquid phase separation can initiate tau aggregation. *EMBO J.* **37**, e98049 (2018).
26. Wortmann, P., Götz, M. & Hugel, T. Cooperative Nucleotide Binding in Hsp90 and Its Regulation by Aha1. *Biophys. J.* **113**, 1711–1718 (2017).
27. Schmid, S., Götz, M. & Hugel, T. Effects of Inhibitors on Hsp90's Conformational Dynamics, Cochaperone and Client Interactions. *ChemPhysChem* **19**, 1716–1721 (2018).
28. Diablerets, L., Picard, D. & Buchner, J. The Hsp90 Chaperone Machine. (2010).
29. Mishra, P. & Bolon, D. N. A. Designed Hsp90 heterodimers reveal asymmetric ATPase-driven mechanism in vivo. *Mol. Cell* **53**, 344 (2014).
30. Li, J., Soroka, J. & Buchner, J. The Hsp90 chaperone machinery: Conformational dynamics and regulation by co-chaperones. *Biochim. Biophys. Acta - Mol. Cell Res.* **1823**, 624–635 (2012).
31. Buchner, J. & Li, J. Structure, Function and Regulation of the Hsp90 Machinery. *Biomed. J.* **36**, 106 (2013).
32. Agam, G. *et al.* Reliability and accuracy of single-molecule FRET studies for characterization of structural dynamics and distances in proteins. *Nat. Methods* **20**, 523–535 (2023).
33. Wilmes, S. *et al.* Mechanism of homodimeric cytokine receptor activation and dysregulation by oncogenic mutations. *Science (80-.).* **367**, 643–652 (2020).
34. Makio Tokunaga, N. I. & K. S.-S. Highly inclined thin illumination enables clear single-molecule imaging in cells. **5**, 1–7 (2010).
35. Ha, T. Single-molecule fluorescence resonance energy transfer. *Methods* **25**, 78–86 (2001).
36. Kapanidis, A. N. *et al.* Alternating-Laser Excitation of Single Molecules. *Acc. Chem. Res.* **38**, 523–533 (2005).
37. Kapanidis, A. N. *et al.* Retention of transcription initiation factor σ70 in transcription elongation: Single-molecule analysis. *Mol. Cell* **20**, 347–356 (2005).
38. Kong, X., Nir, E., Hamadani, K. & Weiss, S. Photobleaching pathways in single-molecule FRET experiments. *J. Am. Chem. Soc.* **129**, 4643–4654 (2007).
39. Quel, N. G. *et al.* Heat shock protein 90 kDa (Hsp90) from Aedes aegypti has an open conformation and is expressed under heat stress. *Int. J. Biol. Macromol.* **156**, 522–530 (2020).
40. Ali, M. M. U. *et al.* Crystal structure of an Hsp90–nucleotide–p23/Sba1 closed chaperone

complex. *Nat. 2006 4407087* **440**, 1013–1017 (2006).
41. Zen, K., Biwersi, J., Periasamy, N. & Verkman, A. S. Second messengers regulate endosomal acidification in Swiss 3T3 fibroblasts. *J. Cell Biol.* **119**, 99–110 (1992).
42. Tsien, R. Y. Chapter 5 Fluorescent Indicators of Ion Concentrations. *Methods Cell Biol.* **30**, 127–156 (1989).
43. Seksek, O., Biwersi, J. & Verkman, A. S. Direct measurement of trans-Golgi pH in living cells and regulation by second messengers. *J. Biol. Chem.* **270**, 4967–4970 (1995).
44. Monnier, N. *et al.* Inferring transient particle transport dynamics in live cells. *Nat. Methods 2015 129* **12**, 838–840 (2015).
45. Martens, K. J. A. *et al.* Visualisation of dCas9 target search in vivo using an open-microscopy framework. *Nat. Commun. 2019 101* **10**, 1–11 (2019).
46. López, A., Elimelech, A. R., Klimm, K. & Sattler, M. The Charged Linker Modulates the Conformations and Molecular Interactions of Hsp90. *ChemBioChem* **22**, 1084–1092 (2021).
47. Jahn, M. *et al.* The charged linker of the molecular chaperone Hsp90 modulates domain contacts and biological function. *Proc. Natl. Acad. Sci. U. S. A.* **111**, 17881–17886 (2014).
48. Tsutsumi, S. *et al.* Charged linker sequence modulates eukaryotic heat shock protein 90 (Hsp90) chaperone activity. *Proc. Natl. Acad. Sci. U. S. A.* **109**, 2937–2942 (2012).
49. Götz, M., Wortmann, P., Schmid, S. & Hugel, T. A Multicolor Single-Molecule FRET Approach to Study Protein Dynamics and Interactions Simultaneously. *Methods Enzymol.* **581**, 487–516 (2016).
50. Goulian, M. & Simon, S. M. Tracking Single Proteins within Cells. *Biophys. J.* **79**, 2188–2198 (2000).
51. Plochowietz, A., El-Sagheer, A. H., Brown, T. & Kapanidis, A. N. Stable end-sealed DNA as robust nano-rulers for in vivo single-molecule fluorescence. *Chem. Sci.* **7**, 4418–4422 (2016).
52. Schmid, S., Götz, M. & Hugel, T. Single-Molecule Analysis beyond Dwell Times: Demonstration and Assessment in and out of Equilibrium. *Biophys. J.* **111**, 1375–1384 (2016).
53. Schrangl, L. Single-molecule FRET analysis software. (2021). doi:10.5281/ZENODO.4604567
54. Schrangl, L. *et al.* Automated Two-dimensional Spatiotemporal Analysis of Mobile Single-molecule FRET Probes. *JoVE (Journal Vis. Exp.* **2021**, e63124 (2021).
55. Gao, Y. *et al.* Accurate detection and complete tracking of large populations of features in three dimensions. *Opt. Express, Vol. 17, Issue 6, pp. 4685-4704* **17**, 4685–4704 (2009).
56. Schrangl, L. sdt-python: Python library for fluorescence microscopy data analysis (v17.5). *Zenodo* (2023). doi:10.5281/ZENODO.7616161
57. Wortmann, P., Götz, M. & Hugel, T. Cooperative Nucleotide Binding in Hsp90 and Its Regulation by Aha1. *Biophys. J.* **113**, 1711 (2017).
58. Lee, N. K. *et al.* Accurate FRET measurements within single diffusing biomolecules using alternating-laser excitation. *Biophys. J.* **88**, 2939–2953 (2005).